

Supporting Information (SI)

Protein Particles Decorated with Pd Nanoparticles for the Catalytic Reduction of p-Nitrophenol to p- Aminophenol

Yeonhwa Yu,^{1,†} Euiyoung Jung,^{2,3,†} Hyun Jin Kim,¹ Ahyoung Cho,² Jinheung Kim,³ Taekyung Yu^{2,} and Jeewon Lee^{1,*}*

¹Department of Chemical and Biological Engineering, College of Engineering, Korea University, Anam-Ro 145, Seoul 136-713, Republic of Korea

² Department of Chemical Engineering, College of Engineering, Kyung Hee University, Yongin 17104, Republic of Korea

³Department of Chemistry and Nano Science, Ewha Womans University, Seoul 03760, Republic of Korea

*Correspondence to: leejw@korea.ac.kr (J.L.), tkyu@khu.ac.kr (T.Y.).

†These authors contributed equally.

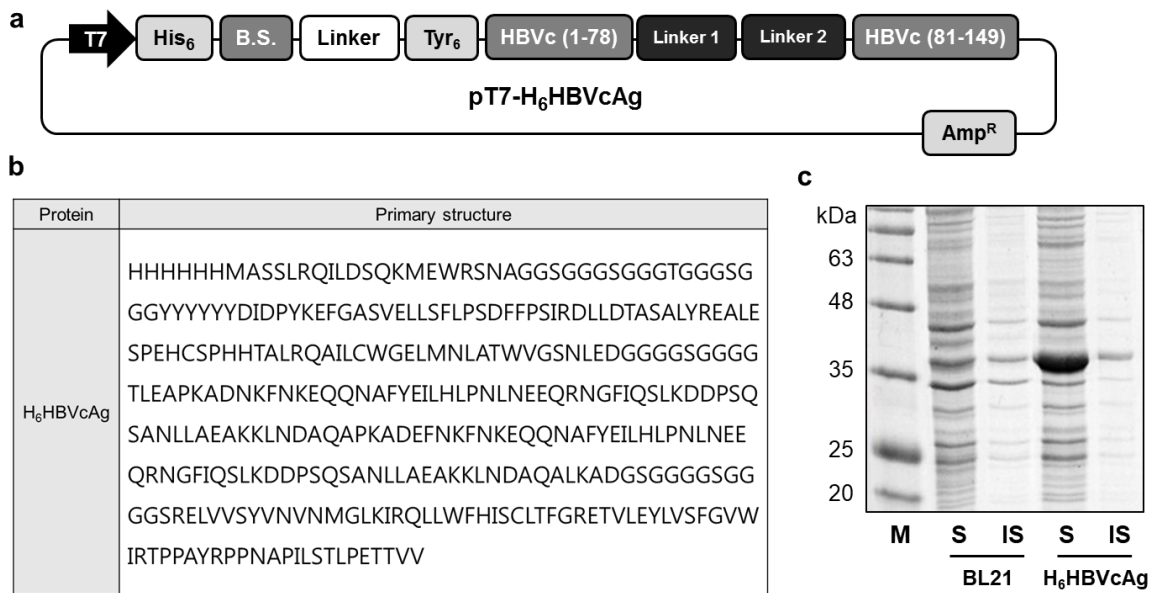


Figure S1. Plasmid expression vector (a) and coding sequence (b) for H₆HBVcAg and (c) result of SDS-PAGE analysis of soluble (S) and insoluble fraction (IS) recombinant *E. coli* cell lysates producing H₆HBVcAg.

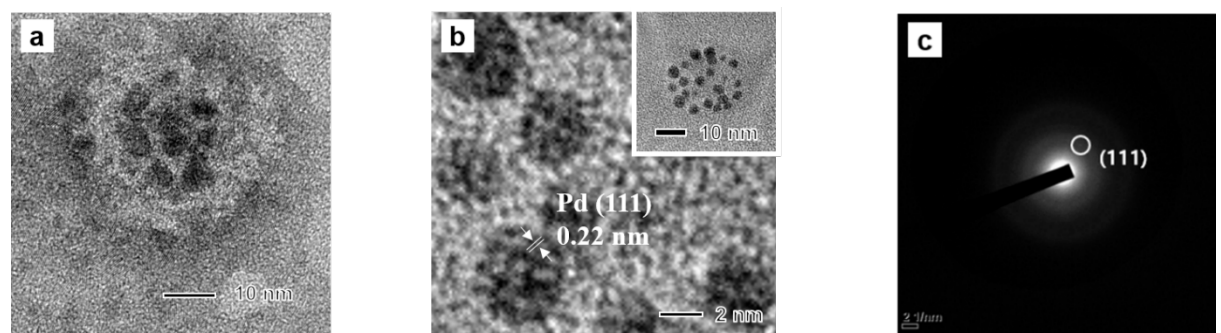


Figure S2. (a) Stained TEM image, (b) unstained HRTEM image (inset : unstained TEM image), and (c) ED pattern of PdNP-PPs.

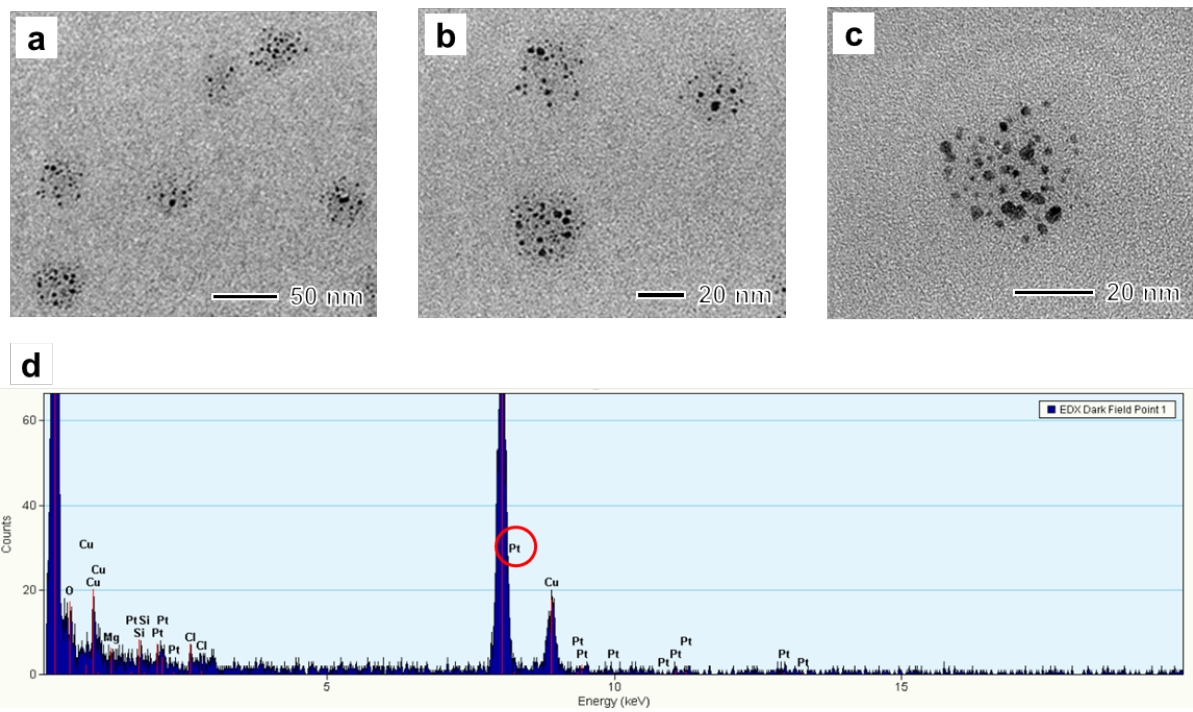


Figure S3. (a-c) TEM images and (d) EDX spectrum of samples synthesized by sequential addition of Pt precursor and Pd precursor.

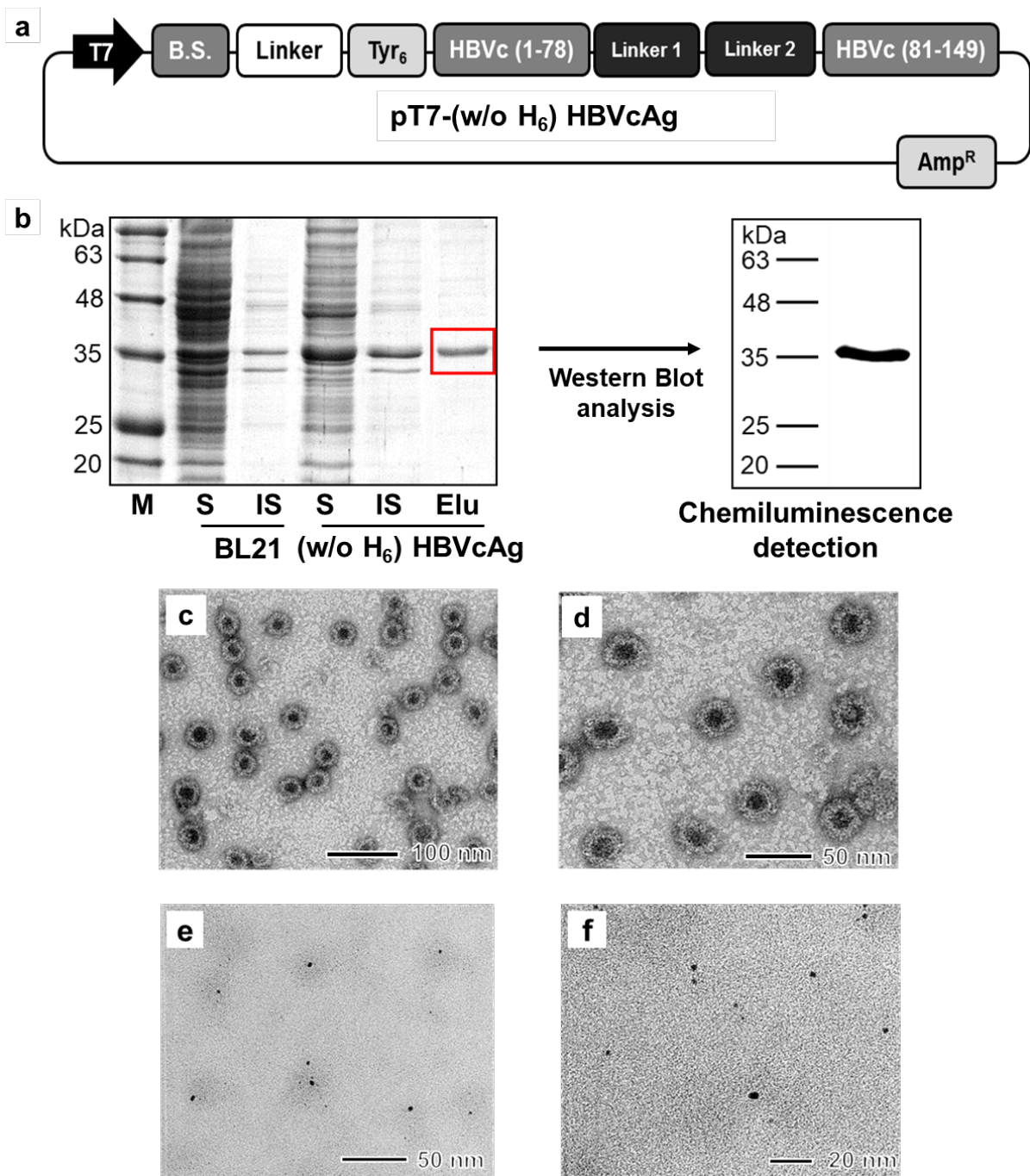


Figure S4. (a) Plasmid expression vector for (w/o H₆) HBVcAg, (b) result of SDS-PAGE analysis and Western blot analysis, (c-d) TEM images of (w/o H₆) HBVcAg PPs and (e-f) TEM images of PdNP-PPs using the (w/o H₆) HBVcAg PPs.

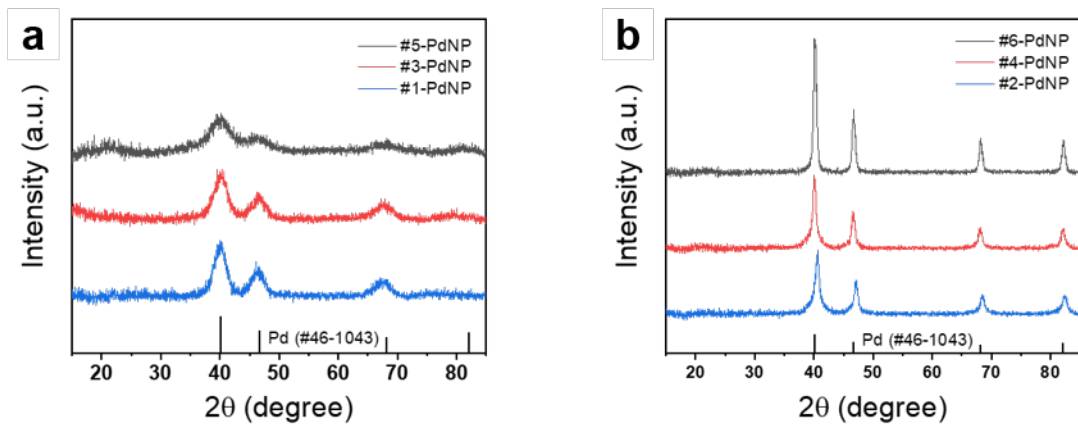


Figure S5. XRD diffraction patterns of (a) PdNPs (~ 3 nm) and (b) PdNPs (~ 30 nm).

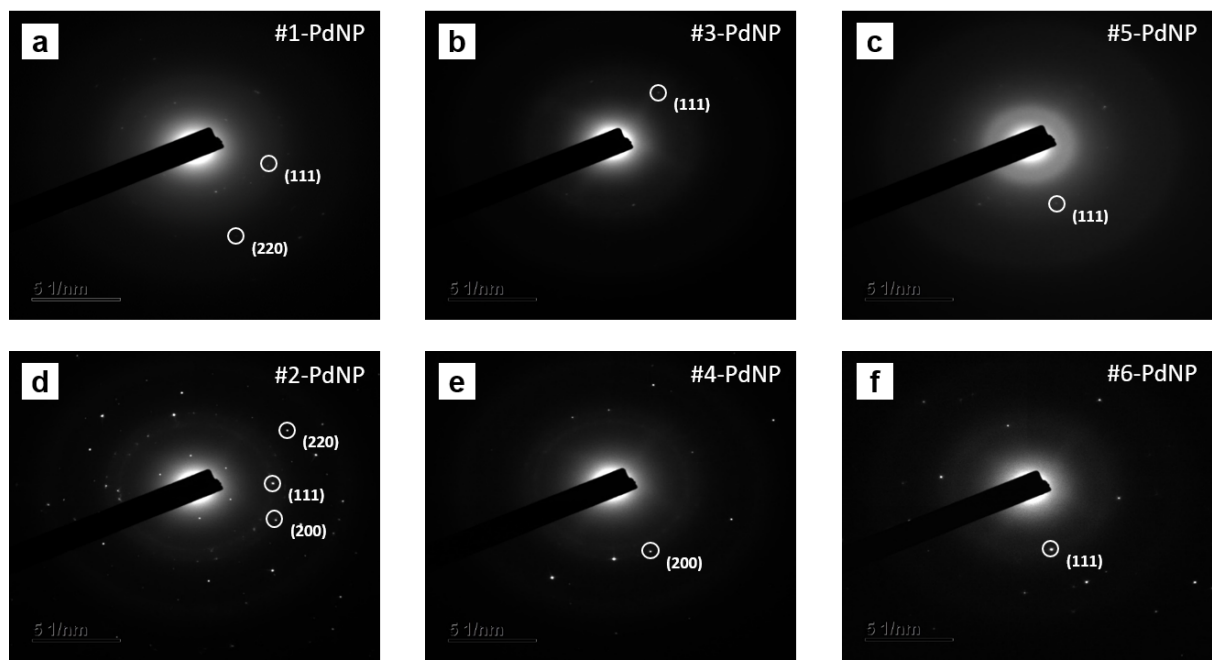


Figure S6. ED patterns of (a) #1-PdNP, (b) #3-PdNP, (c) #5-PdNP, (d) #2-PdNP, (e) #4-PdNP, and (f) #6-PdNP.

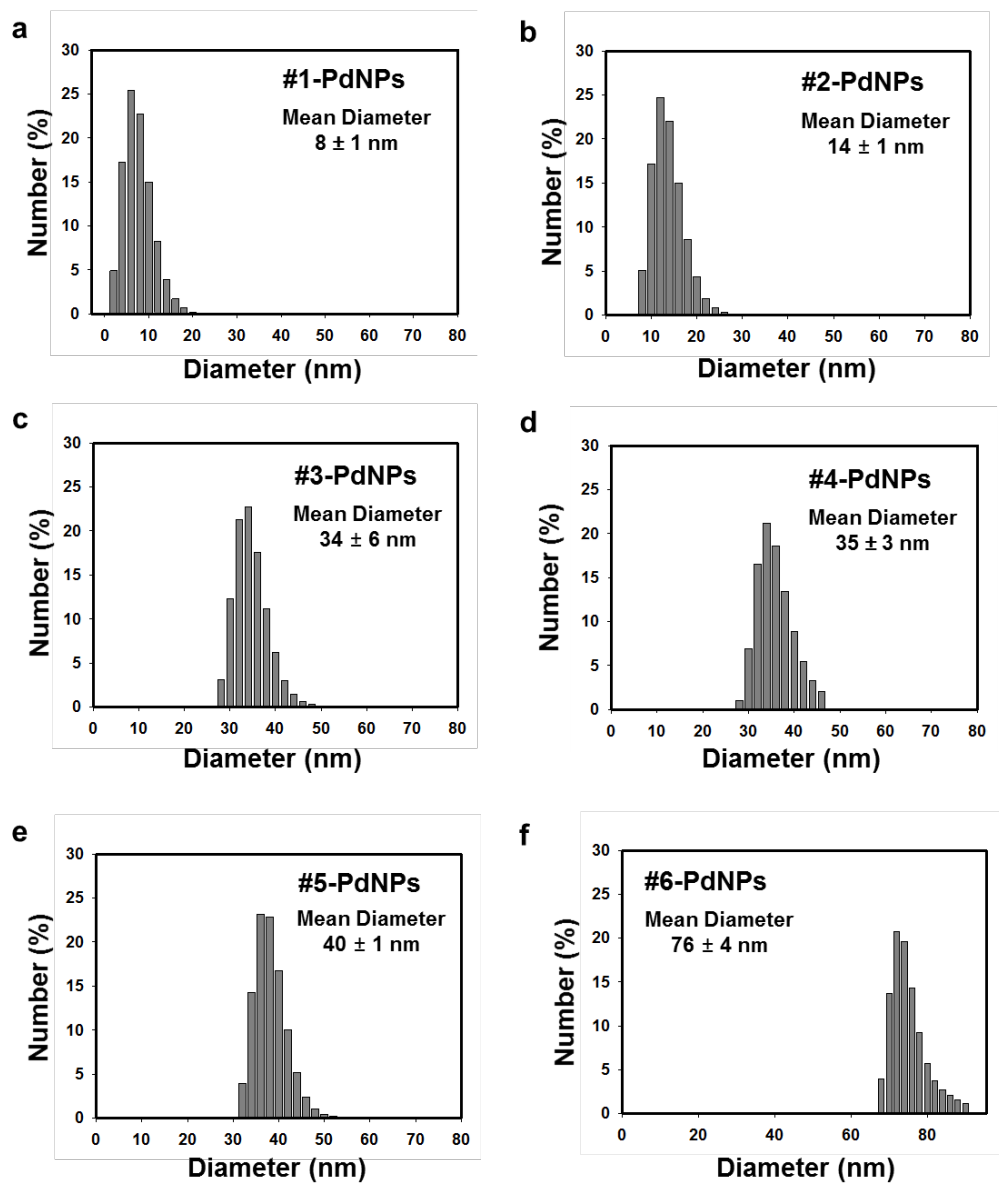


Figure S7. Results of DLS (a-f) and zeta potential (g) analyses of #1- to #6-PdNPs.

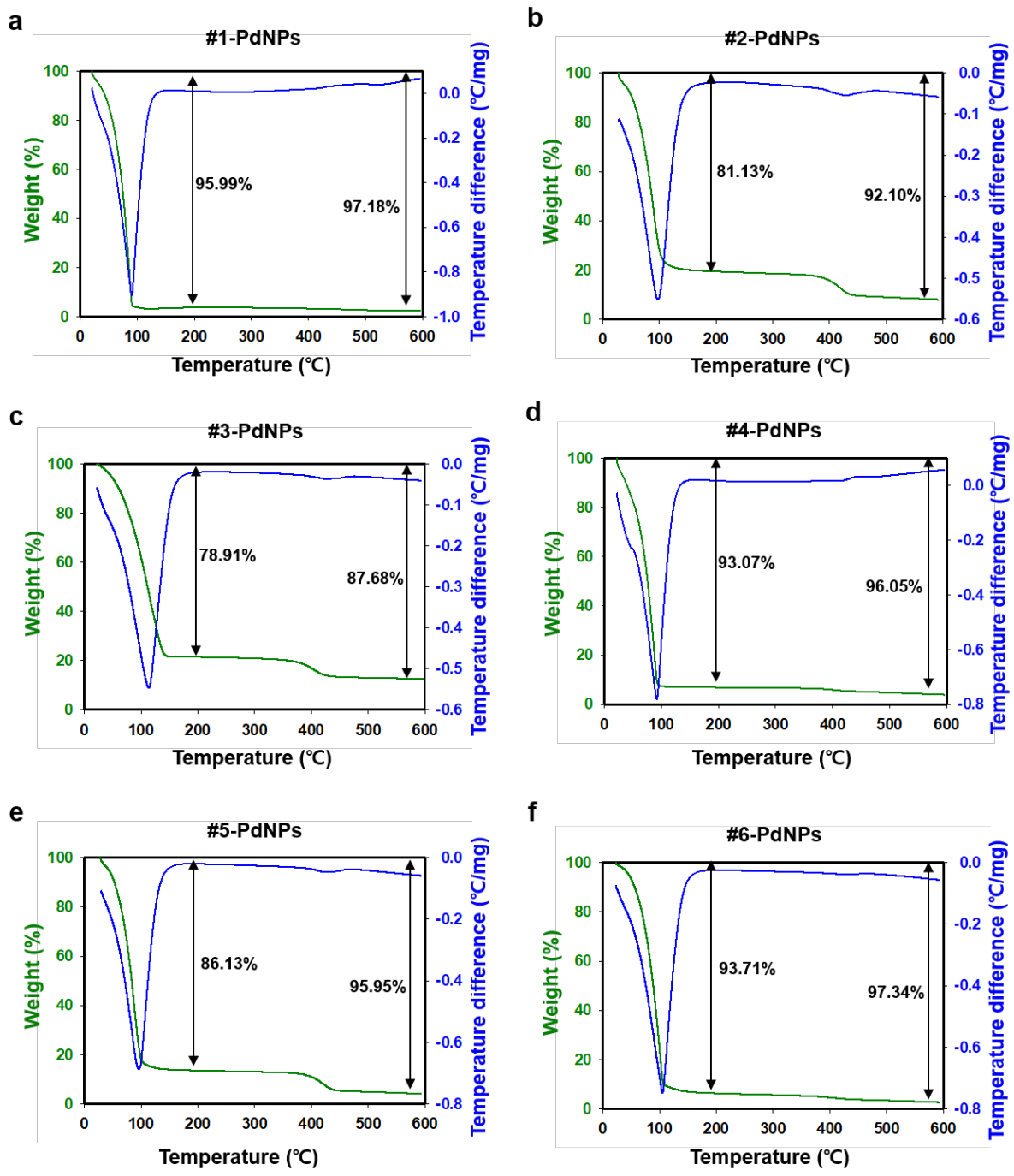


Figure S8. Results of TG-DTA analysis of PdNPs.

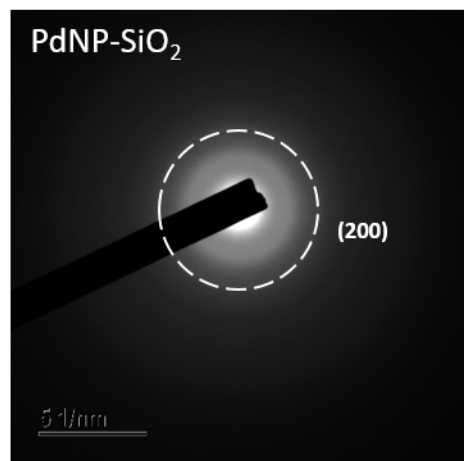


Figure S9. ED patterns of PdNP-SiO₂.

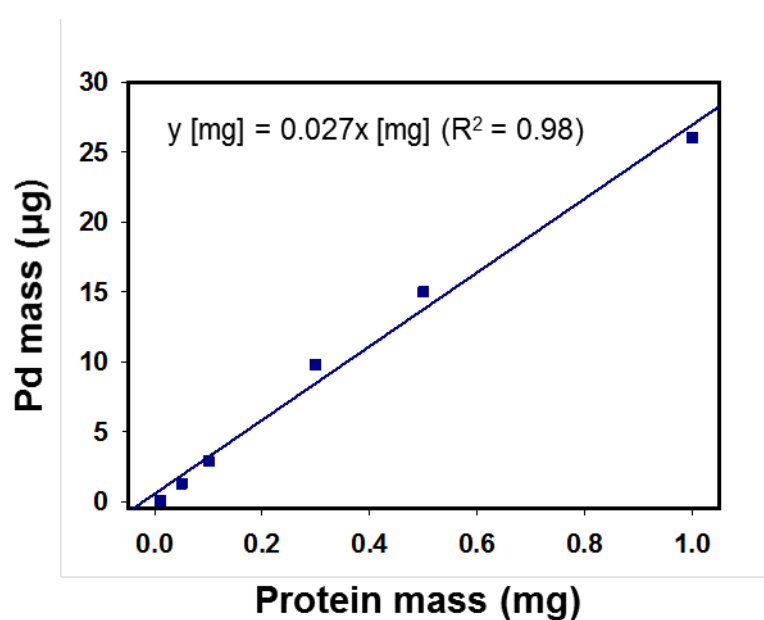
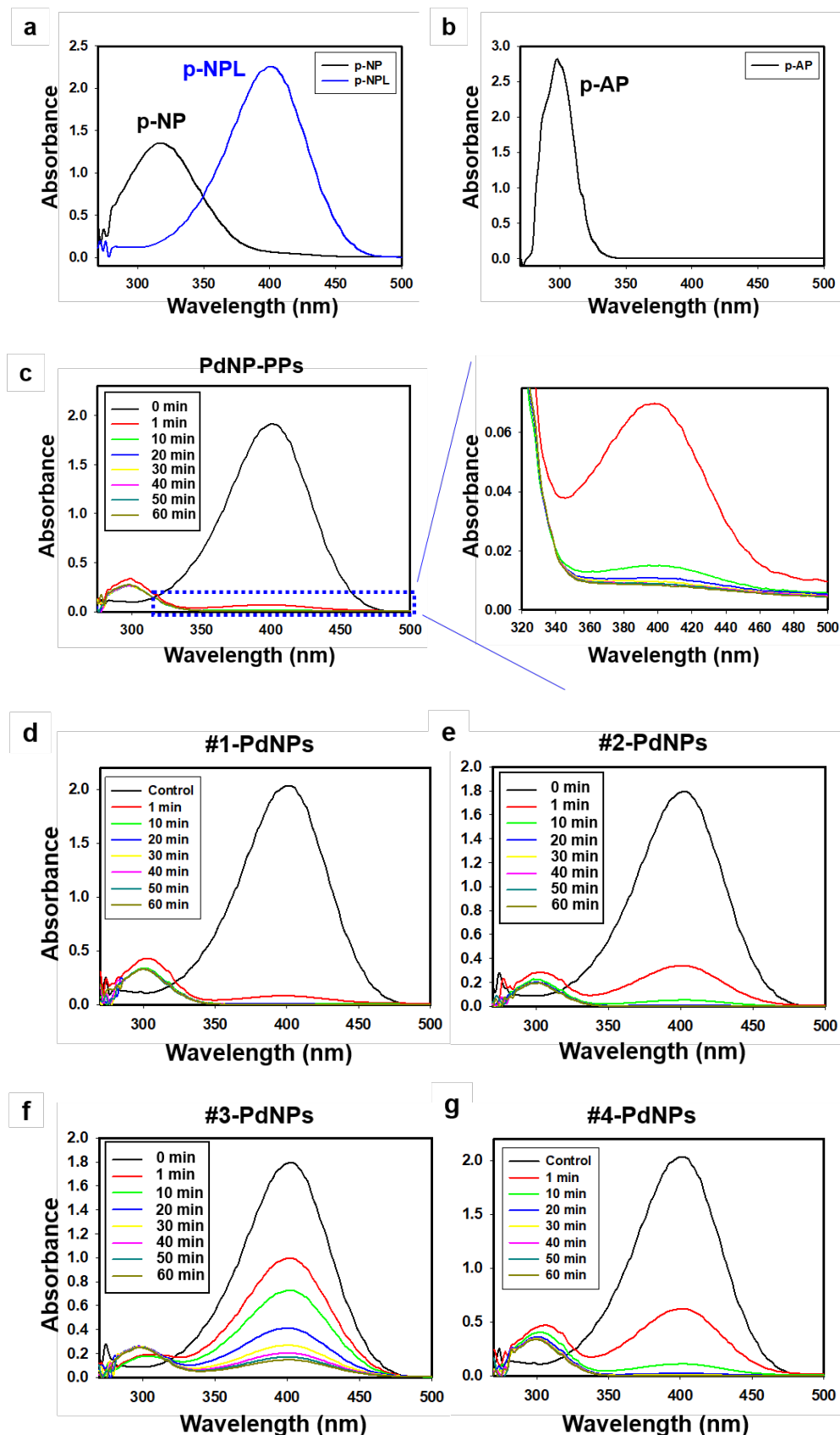


Figure S10. Correlation between Pd mass and protein mass in PdNP-PPPs, determined by ICP-MS analysis.



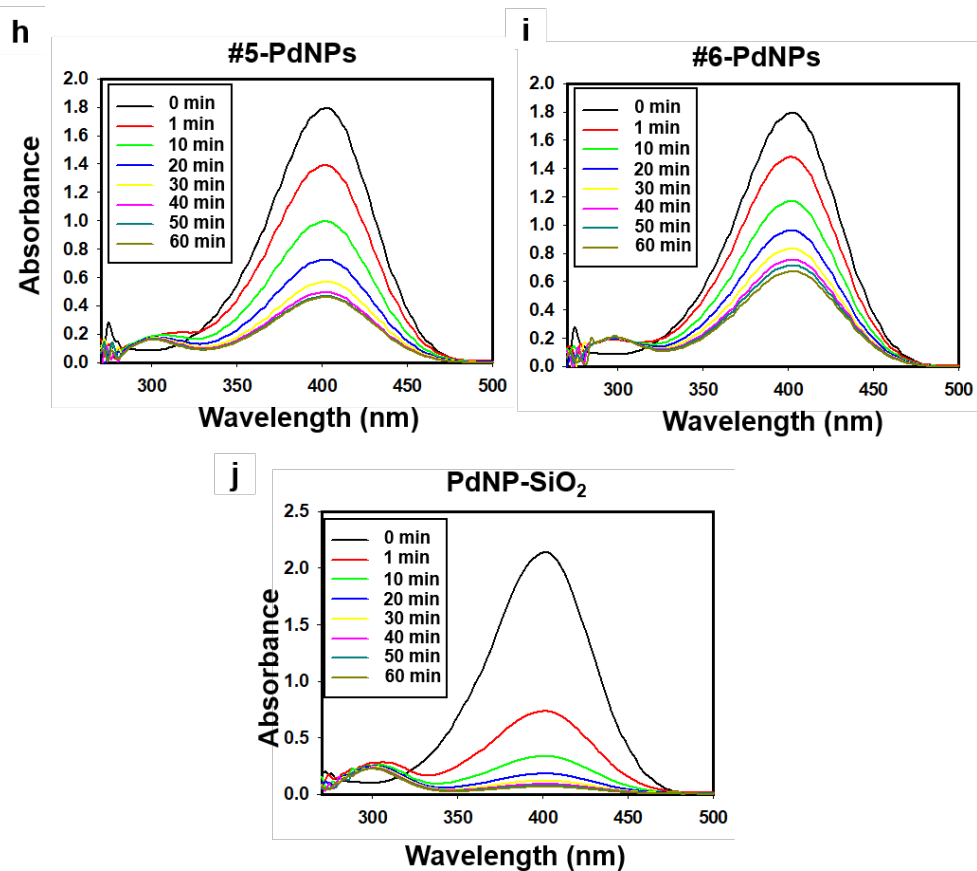


Figure S11. Maximum absorption peaks for (a) p-NP and p-NPL, (b) p-AP, and time-course changes in maximum absorption peaks for p-NPL and p-AP during the reduction of p-NPL to p-AP using various Pd nanocatalysts: (c) PdNP-PPs, (d) #1-PdNPs, (e) #2-PdNPs, (f) #3-PdNPs, (g) #4-PdNPs, (h) #5-PdNPs, (i) #6-PdNPs, and (j) PdNP-SiO₂.

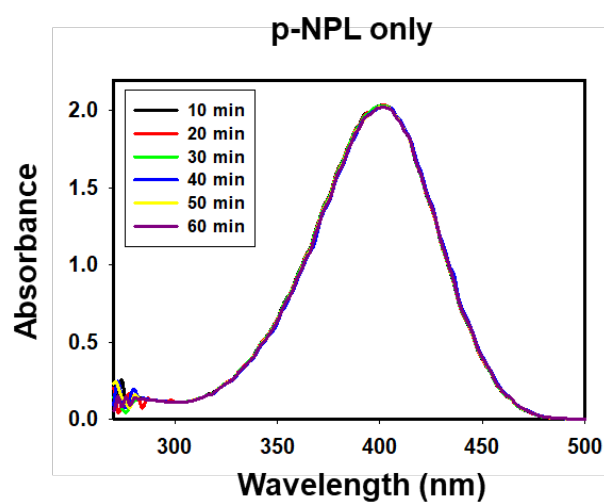
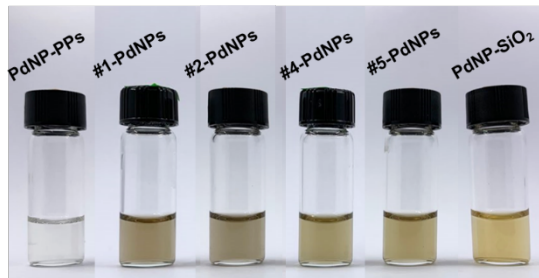


Figure S12. UV-vis spectra of an aqueous solution containing p-nitrophenol and NaBH₄ without the Pd catalysts during 60 min.

Before the 1st cycle



After the last cycle

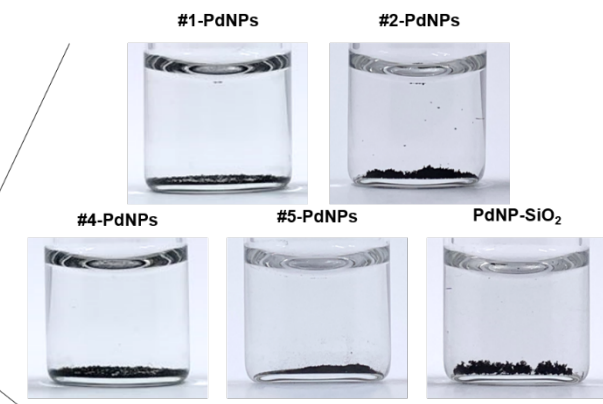
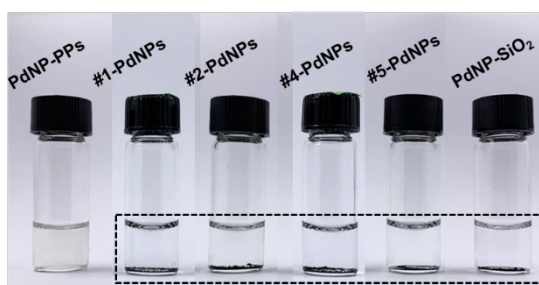


Figure S13. Photographic images of various Pd nanocatalysts solutions, collected before the 1st cycle and after the last cycle of multi-cyclic reactions.

Table S1. The TON and TOF values of Pd nanocatalysts during the recyclability tests.

	Cycle	1	2	3	4	5
PdNP-PPs	TON	57.7	56.4	55.5	52.2	47.2
	TOF(min ⁻¹)	5.8	5.6	5.5	5.2	4.7
PdNP-SiO₂	TON	35.7	18.2	10.3	6.9	9.5
	TOF(min ⁻¹)	3.6	1.8	1.0	0.7	0.9
#3-PdNPs (Pd 3 nm w/ 40000 MW PVP)	TON	55.5	6.5	4.1	4.6	3.0
	TOF(min ⁻¹)	5.6	0.6	0.4	0.5	0.3
#4-PdNPs (Pd 30 nm w/ 40000 MW PVP)	TON	39.4	3.9	3.8	3.0	2.5
	TOF(min ⁻¹)	3.9	0.4	0.4	0.3	0.3
#5-PdNPs (Pd 3 nm w/ 10000 MW PVP)	TON	57.4	56.1	22.3	22.4	8.6
	TOF(min ⁻¹)	5.7	5.6	2.2	2.2	0.9
#6-PdNPs (Pd 30 nm w/ 10000 MW PVP)	TON	53.9	29.9	30.2	7.2	6.9
	TOF(min ⁻¹)	5.4	3.0	3.0	0.7	0.7

Table S2. Amino acids and their binding metal ions.

Amino acid	Metal ions	Reference
Histidine	Pd ²⁺ , Zn ²⁺ , Cd ²⁺ , Cu ²⁺ , Ni ²⁺ , Ag ⁺	1-6
Cysteine	Hg ²⁺ , Pb ²⁺ , Zn ²⁺ , Cd ²⁺	6-8
Tryptophan	Cu ²⁺	6, 9
Tyrosine	Fe ³⁺ >Co ²⁺ >Ni ²⁺ >Cu ²⁺ (binding affinity)	10

Table S3. Catalytic activity comparison of PdNP-PPs with other Pd catalysts.

Catalyst	Metal size (nm)	Mass of catalyst (mg)	Concentration of p-NP(mM)	Concentration of NABH ₄ (mM)	TOF (mmol p-NP/ mmol metal min)	Reference
PdNP-PPs	3				5.8	
PVP(10000 MW)- Pd	3 / 30	0.81 × 10 ⁻⁴	0.2	33.3	5.7 / 5.4	This study
PdNP-SiO ₂	3				3.6	
Pd@h-mSiO ₂ - 4.9%		0.05	0.1	8.3	1.56	11
CNT/PiHP/Pd	2.1 - 31.6	0.3 × 10 ⁻⁵	0.2	16.5	1.5	12
RGO@Pd@C	4	5	0.1	19.4	4.6	13
Pd-rGO-CNT	4	5	0.1	9.7	1.2	14

References

1. Learte-Aymamí, S.; Vidal, C.; Gutiérrez-González, A.; Mascareñas, J. L. Intracellular Reactions Promoted by Bis(histidine) Miniproteins Stapled Using Palladium(II) Complexes *Angew. Chem. Int. Ed.*, **2020**, *59*, 9149-9154.
2. Morgan, D. M.; Dong, J.; Jacob, J.; Lu, K.; Apkarian, R. P.; Thiagarajan, P.; Lynn, D. G. Metal Switch for Amyloid Formation: Insight into the Structure of the Nucleus. *J. Am. Chem. Soc.* **2002**, *124*, 12644-12645.
3. Dong, J.; Shokes, J. E.; Scott, R. A.; Lynn, D. G. Modulating Amyloid Self-Assembly and Fibril Morphology with Zn(II). *J. Am. Chem. Soc.* **2011**, *133*, 19993-20000.
4. Sóvágó, I.; Ősz, K. Metal Ion Selectivity of Oligopeptides. *Dalton Trans.*, **2006**, *32*, 3841-3854.
5. Yang, H.; Pritzker, M.; Fung, S. Y.; Sheng, Y.; Wang, W.; Chen, P. Anion Effect on the Nanostructure of a Metal Ion Binding Self-Assembling Peptide. *Langmuir* **2006**, *22*, 8553-8562.
6. Zou, R.; Wang, Q.; Wu, J.; Wu, J.; Schmuck, C.; Tian, H. Peptide Self-Assembly Triggered by Metal Ions. *Chem. Soc. Rev.* **2015**, *44*, 5200-5219.
7. Kikot, P.; Polat, A.; Achilli, E.; Lahore, M. F.; Grasselli, M. Immobilized Palladium(II) Ion Affinity Chromatography for Recovery of Recombinant Proteins with Peptide Tags Containing Histidine and Cysteine. *J. Mol. Recognit.*, **2014**, *27*, 659-668.
8. Dieckmann, G. R.; McRorie, D. K.; Lear, J. D.; Sharp, K. A.; DeGrado, W. F.; Pecoraro, V. L. The Role of Protonation and Metal Chelation Preferences in Defining the Properties of Mercury-Binding Coiled Coils. *J. Mol. Biol.* **1998**, *280*, 897-912.
9. Ghosh, S.; Singh, P.; Verma, S. Morphological Consequences of Metal Ion-Peptide Vesicle Interaction. *Tetrahedron* **2008**, *64*, 1250-1256.
10. Singh, R.; Mishra, N. K.; Kumar, V.; Vinayak, V.; Joshi, K. B. Transition Metal Ion-Mediated Tyrosine-Based Short-Peptide Amphiphile Nanostructures Inhibit Bacterial Growth. *ChemBioChem* **2018**, *19*, 1630-1637.
11. Tian, M.; Long, Y.; Xu, D.; Wei, S.; Dong, Z. Hollow Mesoporous Silica Nanotubes Modified with Palladium Nanoparticles for Environmental Catalytic Applications. *J. Colloid Interface Sci.* **2018**, *521*, 132-140.

12. Li, H.; Han, L.; Cooper-White, J.; Kim, I. Palladium Nanoparticles Decorated Carbon nanotubes: Facile Synthesis and Their Applications as Highly Efficient Catalysts for the Reduction of 4-Nitrophenol. *Green Chem.* **2012**, *14*, 586-591.
13. Zhang, Z.; Xiao, F.; Xi, J.; Sun, T.; Xiao, S.; Wang, H.; Wang, S.; Liu, Y. Encapsulating Pd Nanoparticles in Double-Shelled Graphene@Carbon Hollow Spheres for Excellent Chemical Catalytic Property. *Sci. Rep.* **2014**, *4*, 4053.
14. Sun, T.; Zhang, Z.; Xiao, J.; Chen, C.; Xiao, F.; Wang, S.; Liu, Y. Facile and Green Synthesis of Palladium Nanoparticles-Graphene-Carbon Nanotube Material with High Catalytic Activity. *Sci. Rep.* **2013**, *3*, 2527.